

General Disclaimer

One or more of the Following Statements may affect this Document

- This document has been reproduced from the best copy furnished by the organizational source. It is being released in the interest of making available as much information as possible.
- This document may contain data, which exceeds the sheet parameters. It was furnished in this condition by the organizational source and is the best copy available.
- This document may contain tone-on-tone or color graphs, charts and/or pictures, which have been reproduced in black and white.
- This document is paginated as submitted by the original source.
- Portions of this document are not fully legible due to the historical nature of some of the material. However, it is the best reproduction available from the original submission.

NSG-1231



SOCIETY OF AUTOMOTIVE ENGINEERS, INC.
400 Commonwealth Drive, Warrendale, Pa. 15096

Flight Test Evaluation of a Method to Determine the Level Flight Performance of a Propeller-Driven Aircraft

Phillip D. Bridges, Dr. Ernest J. Cross, Jr.,
and Donald W. Boatwright

Mississippi State University

Society of Automotive Engineers

Business Aircraft Meeting
Century II, Wichita
March 29 - April 1, 1977

770470

Flight Test Evaluation of a Method to Determine the Level Flight Performance of a Propeller-Driven Aircraft

*Phillip D. Bridges, Dr. Ernest J. Cross, Jr.,
and Donald W. Boatwright

Mississippi State University

DETERMINATION OF THE DRAG OF propeller-driven aircraft in actual flight has long been a problem for the aeronautical engineer. The overall drag of the aircraft is often needed to verify design methods and criteria and to determine the actual propulsive efficiency. Currently, there are two flight test procedures in common use by the general aviation industry which are used to determine aircraft drag. Each of these has significant limitations and associated difficulties.

*Phillip D. Bridges presently employed by
McDonnell Douglas

The use of power-off glide tests to determine the lift-drag coefficient polar is one of the standard methods for experimentally obtaining the drag and span efficiency for conventional aircraft. Because of the feathered-propeller drag and uncertain effects on the drag of the aircraft due to the propeller slip-stream, this method has serious limitations and yields results which are frequently of questionable validity. However, "feathered-sinks" are relatively easy to perform at low cost and alternative methods available do not provide significantly better results. The simplicity of this technique and its proven applicability to sailplanes and small aircraft is well known. However, the method fails to account for airframe-propulsion system

ABSTRACT

A flight test method has been developed for determining the level flight drag and propulsive efficiency of propeller-driven aircraft. The overall drag of the aircraft is expressed in terms of the measured increment of power required to overcome a corresponding known increment of drag, which is generated by a towed drogue. The

simplest form of the governing equations, $D = AD \text{ SHP} / ASHP$, is such that all of the parameters on the right side of the equation can be measured in flight. An evaluation of the governing equations has been performed using data generated by flight test of a Beechcraft T-34B.

interaction effects which may be significant. Thus, a method which would include these effects in a power-on condition is needed.

Propeller effects may be at least partially accounted for by use of the second of the most commonly used methods of flight test drag estimation. In this method, a power required curve is generated for the aircraft in steady, level flight from measurements of propeller shaft torque and rpm, or by means of calibrated engine performance curves. By either method, the drag coefficient of the aircraft is defined as

$$C_D = \frac{550 \eta_p \text{ SHP}}{qSV} \quad (1)$$

where η_p is the propulsive efficiency of the aircraft. This parameter, unfortunately, must usually be determined from generalized empirical data obtained from isolated propeller tests. Since little data have been generated in recent years for small propellers in the general aviation category, most of the information currently available for computing efficiency of these type propellers is outdated. Typical sources of information are those of References 1 and 2 which are based on research conducted over thirty years ago on a class of propellers not representative of contemporary general aviation propellers. Analytical methods such as Reference 3 are available, but because of simplifying assumptions, often yield unacceptable results. Thus, the accuracy of drag determination is directly associated with the accuracy of the propeller charts and analytical methods which are often questionable.

In view of the shortcomings of the gliding flight technique and power-on test method described above, an alternative procedure has been developed in which the effects of uncertainties in propeller efficiency could be minimized or eliminated. This is a method in which the overall drag of the aircraft is expressed in terms of the increment of power required to overcome a known increment of drag. The method is applied to the aircraft in level, unaccelerated flight so that propeller drag and slipstream effects are fully accounted for.

A flight test has been conducted to evaluate the utility of the incremental method of power-on drag measurement. This included not only aircraft operational procedures, but involved the development of instrumentation, trailing drogues and other devices, and data reduction procedures to minimize the effects of errors in flight test data.

THEORY

The propulsive efficiency of a propeller-driven aircraft is defined as

$$\eta_p = \frac{\text{THP}}{\text{SHP}} = \frac{TV}{550\text{SHP}}$$

where η_p is the propulsive efficiency, T is the net thrust acting on the airplane, V is its true velocity in ft/sec, and SHP is the horsepower delivered to the propeller.

In unaccelerated, straight and level flight, the thrust can be expressed in terms of the drag (D), and the thrust inclination angle (γ) such that $T = D/\cos\gamma$ (Figure 1). At normal flight speeds, the thrust inclination angle is small, and the approximation may be made that

$$\eta_p = \frac{DV}{550\text{SHP}} \quad (3)$$

When an increment of drag (ΔD) is added to the aircraft as in Figure 1 and a corresponding amount of power (ΔSHP) is added to maintain the same airspeed and altitude, the propulsive efficiency equation becomes

$$\eta_p + \Delta\eta_p = \frac{(D + \Delta D)V}{550(\text{SHP} + \Delta\text{SHP})} \quad (4)$$

where $\Delta\eta_p$ is the change in propulsive efficiency associated with the change in power.

The drag can be eliminated from Equation (4) by use of Equation (3). Making the substitution gives

$$\eta_p = \frac{\Delta DV}{550\Delta\text{SHP}} - \frac{\Delta\eta_p (\text{SHP} + \Delta\text{SHP})}{\Delta\text{SHP}} \quad (5)$$

A propulsive efficiency ratio can be defined such that

$$E_p = \frac{\eta_p + \Delta\eta_p}{\eta_p} = 1 + \frac{\Delta\eta_p}{\eta_p} \quad (6)$$

Equation (5) can then be written as

$$\eta_p = \frac{\Delta DV}{550[(\text{SHP} + \Delta\text{SHP})E_p - \text{SHP}]} \quad (7)$$

Substitution of this expression for η_p in Equation (3) gives

$$D = \frac{\Delta D}{(1 + \frac{\Delta\text{SHP}}{\text{SHP}})E_p - 1} \quad (8)$$

If the change in propulsive efficiency due to the additional drag (ΔD) is considered to be small, then $E_p \approx 1$ and the drag of the aircraft may be approximated as

$$D = \Delta D \frac{\text{SHP}}{\Delta\text{SHP}} \quad (9)$$

Equation (9) was of considerable interest in the present investigation. The parameters on the right side of the expression can be easily measured, thus permitting the drag of the aircraft to be calculated without the use of empirical or theoretically derived values of propeller efficiency. Instead, once the drag is found, propeller efficiency can be calculated directly from Equation (3). The validity of the

results are directly related to the magnitude of the drag increment used and the corresponding increment of propeller efficiency that is neglected in the evaluation of the equation.

Equation (9) was expected to yield realistic values of drag for certain operating conditions of the aircraft. When the propeller advance ratio is high, propeller efficiency is relatively insensitive to small changes of power as shown in Figure 2. This plot was prepared from Reference 1 for a propeller of the same activity factor as the propeller used in the current investigation. Inspection of this plot indicated that tests should be conducted at advance ratios of $J \geq 0.6$ to minimize propeller efficiency changes. Since only propeller rpm could be adjusted to obtain the higher values of advance ratio over the speed range of the aircraft, all tests were conducted at a propeller speed of 2000 rpm. This speed, which was considered to be the lowest speed consistent with efficient operation of the aircraft, resulted in the desired values of advance ratio at airspeeds above 90 knots.

Equation (8) can be used to compute aircraft drag if the assumption of constant propeller efficiency is not admissible. In this case, some source of propeller data must be available for evaluation of the propeller efficiency ratio, E_p . Although the calculated values of η_p may be questionable, the relative degree of change of these values with power should be fairly accurate if the source data were obtained for a propeller geometrically similar to that of the test aircraft.

There are other potential errors associated with equations (8) and (9) which should be considered. These are errors which are due to failure to account for possible changes in the profile and induced drag of the aircraft produced by the drag increment.

The drag chute which is attached to the fuselage aft end generates a pitching moment about the center of gravity of the aircraft and, the increase of thrust required to overcome the drag increment can also produce a pitching moment. The increased down-load on the tail required to trim the aircraft will result in small changes in the angle of attack of the aircraft which in turn will change the induced and profile drag components of the total drag. For the present work, it was expected that induced drag effects could be significant but profile drag changes of the aircraft could be neglected without appreciable error in the results.

Induced drag effects may be accounted for by considering the change in lift of the aircraft which results from the necessary trim change due to the trailing chute device. The change of induced drag, $(\Delta D)_i$, can be expressed by assuming a parabolic drag polar for the aircraft. Thus,

$$\Delta D_i = \frac{(L + \Delta L)^2 - L^2}{\pi A Re q S} = \frac{2L(\Delta L) + (\Delta L)^2}{\pi A Re q S} \approx \frac{2L(\Delta L)}{\pi A Re q S} \quad (10)$$

The lift increment (ΔL) can be written as

$$L = qS(\Delta C_L) = qS a_0(\Delta \alpha) = qS a_0(\Delta \gamma) \quad (11)$$

Lift can be equated to weight and drag by

$$L = W - T \sin \gamma = W - D \tan \gamma \quad (12)$$

Substituting Equations (11) and (12) into Equation (10) gives

$$\Delta D_i = \frac{2a_0(\Delta \gamma)(W - D \tan \gamma)}{\pi A Re} \quad (13)$$

by letting $\tan \gamma \approx \gamma$

The incremental drag term now can be expressed in terms of both the induced drag increment of Equation (13) and the drag of a trailing chute, ΔD_D . Substitution of these expressions into Equation (8) and neglecting the product $\gamma(\Delta \gamma)$ yields

$$D = \frac{2a_0(\Delta \gamma)W + \pi A Re(\Delta D_D)}{\pi A Re \left[\left(1 + \frac{\Delta SHP}{SHP}\right) E_p - 1 \right]} \quad (14)$$

The incremental drag equation has now become more complex and more difficult to evaluate than the simpler forms derived previously. Although the terms a_0 and "e" are unknown, first approximations of these terms can be used to obtain an initial approximation for the drag. Then, a solution to the equation can be obtained by iteration.

The drogue was attached to the T-34 so that the action-line of the drag was as close as possible to the aircraft center-of-gravity to minimize the induced pitching moments. Several values of the drag increment were used in an effort to evaluate the effects of changes in aircraft induced drag. The maximum drag increment was approximately 10% of the total airplane drag and was selected primarily to be consistent with the assumptions necessary in the development of the governing equations. The minimum drag increment was established by the resolution and sensitivity of the drag-load and engine torque transducers.

EXPERIMENTAL APPARATUS

The test aircraft was a Navy T-34B (Figure 3), manufactured by Beech Aircraft Corporation. The T-34B is an all-metal, low-wing, two-place tandem trainer. It has a constant-speed propeller, retractable landing gear, and is powered by a Continental Model O-470-4. The aircraft was chosen because its size,

performance, and flight characteristics are typical of modern single-engine general aviation aircraft.

The aircraft's standard propeller had been removed previously and replaced with a Hartzell Model FC8468 R propeller. This is a two-bladed, full-feathering propeller with an activity factor of ninety.

An aircraft propeller torque-meter, Model 1308, manufactured by Lebow Associates, Inc., was mounted between the propeller and the aircraft engine (Figure 4). Torque-meter output was measured by a digital transducer indicator Model 7510, also manufactured by Lebow Associates, Inc. This instrument was powered by a 115 VAC, 60 Hz inverter and was calibrated to display the output in foot-pounds. Engine torque was recorded directly by the rear seat observer.

An electronic counter was used to measure the propeller speed directly by means of a magnetic pickup on the aircraft magneto. Pulse signals from the magneto were counted by a Hewlett-Packard Model 5301 counter and displayed in digital form. By directly counting the propeller rpm, as opposed to using an analog output, an accuracy of ± 4 rpm was achieved. Rear seat instrumentation including the torque-meter and rpm counter is shown in Figure 5.

A number of drogues were developed and evaluated for use as possible trailing drag devices. These drogues were sized to provide drag increments of approximately 10 percent of the total airplane drag. Sketches of the devices tested are illustrated in Figures 6, 7, and 8. Best performance was obtained with the bucket-type configuration. The other shapes were unsatisfactory, primarily, due to unstable flight and correspondingly large drag excursions. The stable configuration was essentially cylindrical in shape and was made of light cotton fabric. The leading edge consisted of a 3/16-inch aluminum rod formed into a circle. The trailing end of the drogue was reefed with a drawstring to form a 4-inch diameter vent to control the drag and make it stable over the performance envelope of the test airplane.

Tests of both nylon lines and steel tow cables were conducted to determine the effect of the weight and elasticity of the tow lines on the drag measurements and flight characteristics of the drogues. Possible effects of the aircraft wake on the drogues was also investigated by tests using both 40- and 80-foot tow lines. Comparisons of the drogue data revealed no measurable effects on the drag of these devices due to tow line length or type. The final flight configuration selected for tests consisted of the aircraft towing a bucket-type drogue with a 40-foot, 1/32-inch diameter, steel multistrand cable (Figure 9).

The drag increment generated by the drogue was measured with a Gould, Inc., load cell Model UL 4-50 in series with the drogue and air-

plane. The load cell was mounted to the airplane aft fuselage bulkhead as shown in Figure 10 by a universal joint so that the drogue force vector acted along the load axis of the transducer. Further, the drogue line was fitted with a heavy-duty swivel to avoid line twisting. The load cell attachment fitting was mechanized so that the drogue could be released in flight by the pilot just prior to touchdown. The drogue was attached and fully-deployed prior to take-off. The output voltage of the load cell (5mv maximum) was amplified by a factor of 40 and displayed on two Datal digital panel meters. One was mounted in the rear cockpit and the other in a photopanel which provided the time history of the drogue drag during the flight test and provided a permanent record of the data.

The aircraft flight variables were measured with special probes and sensors. Aircraft dynamic pressure and local static pressure were measured using a self-aligning probe which was mounted at the left wingtip on a rigid boom (Figure 11). Two radial potentiometers were incorporated within the probe in such a way that pitch and side-slip angles could be measured.

The outside air temperature was measured by a probe located under the left wing (Figure 12). The sensing element was a Model 35J3 thermistor manufactured by Omega Engineering, Inc., and was mounted in an appropriate radiation shield.

The photopanel, (Figure 13), was mounted in the aircraft baggage compartment and served as the primary data acquisition system. It contained a clock, altimeter, airspeed indicator, panel voltmeter, and a binary-display light system which was used as an event marker. The loadcell and outside air thermistor output voltages were processed through a two-channel multiplexer and displayed on the panel meter. A small light mounted in the upper left of the panel was used as a signal discriminator for the two output voltages.

The panel was illuminated by six 12-watt bulbs and photographed with a 16mm movie camera using Kodak Tri-X Reversal (ASA 160) film at a rate of 1 frame per second. The camera was controlled by an on-off switch located in the pilot's compartment.

A schematic of the electrically-powered instruments and the associated power system is shown in Figure 14. All AC power was provided by an inverter powered by the 24-volt aircraft battery. The 115 VAC, 60 Hz output was wired to a four-plug junction box. This became the central source for all AC instruments and the five-volt DC power supply for the angle of attack probe and the Datal digital panel meters.

The data system was designed specifically for simplicity and low cost. Each of the sensors is off-the-shelf, and, they are virtually standard equipment in most general aviation flight test organizations.

FLIGHT TEST PROCEDURE AND DATA REDUCTION

A flight test procedure was established to generate speed-power data for the aircraft in both the clean configuration and with a trailing drogue. All flights were in calm air to minimize the spurious effects of atmospheric turbulence. The data were reduced to standard sea level conditions and an aircraft weight standard to facilitate evaluation of the incremental drag equations.

The measured flight test variables consisted of indicated airspeed and pressure altitude, outside air temperature, incremental drag value, propeller speed, engine torque, and angle of attack. Airspeed, altitude, air temperature, and incremental drag were determined as time-averaged values from photopanel data. Engine torque, propeller speed, and angle of attack were recorded by the flight observer. Aircraft weight at each test condition was computed from take-off gross weight and a flight-averaged fuel consumption.

Each test point comprised a minimum data run of 30 seconds stable flight. The speed stability characteristics of the test aircraft were such that stable conditions were virtually impossible to establish for indicated speeds between stall and approximately 80 knots. The speed-power data in this range have excessive and unacceptable scatter, therefore, all performance calculations were based on flight speeds above 80 to 90 knots. The maximum level speed possible with a drogue was typically 110 knots. This was a severe performance limitation and restrained a full evaluation of the test method since the available speed range was only 20 knots. Test points were in 5 knot intervals, approximately, over the available level speed envelope of the airplane. Test points were established by varying the engine torque in small increments at 2000 rpm and waiting for the aircraft speed to stabilize for each data run.

The data were digitized and processed on a UNIVAC 1106 computer. This program, which is listed in the Appendix, computes values of generalized velocity (VIW), generalized power (PIW), equivalent airspeed (V_e), dynamic pressure (q), and chute drag (ΔD) at each test speed. A standard aircraft weight of 3000 pounds was selected for the generalized data.

A functional relationship was determined from the speed-power data for each configuration to facilitate drag computations and analyses. A curve of the form

$$PIW = A(VIW)^3 + B(VIW)^{-1}$$

was fitted to the data points by using a least squares routine for evaluation of the constants A and B. All of the flight test data is presented, however, only data at 90 knots and higher were used to evaluate the functional

constants. These data and corresponding curves are shown in Figures 15 through 18.

Similarly, the drogue drag data were plotted and a linear function of the dynamic pressure assumed such that

$$\Delta D = Aq + B$$

The constants were computed by a least squares method again which resulted in correlation factors of .99 or better. Figure 19 shows the flight test data and appropriate curves for three different bucket-type drogues.

DISCUSSION OF RESULTS

The initial effort to evaluate the incremental drag concept was directed to Equation (9), the simplest and most easily evaluated of the incremental drag equations. In this expression, changes in propeller efficiency and induced drag due to the addition of a drag increment to the aircraft are assumed negligible. Thus, Equation (9) could be evaluated directly from the generalized power curves of the aircraft and plots of drogue drag. These data were obtained for the clean aircraft and for the aircraft towing the 8, 10, and 12-inch diameter bucket-type drogues shown in Figures 6 and 7.

Aircraft drag was calculated at flight speeds from 90 to 110 knots by using the equations for power and drogue drag that were obtained from the curve fits to the experimental data. These equations and the aircraft drag values calculated from Equation (9) are presented in Table 1. The corresponding plots of aircraft drag coefficient (C_D versus C_L^2) shown in Figure 22 were almost linear, indicating a near parabolic drag polar for the aircraft, however, the results obtained from the 8, 10, and 12-inch diameter drogue data were markedly different.

It was expected that the computed aircraft drag coefficients would differ only slightly from those obtained in gliding flight, power-off and propeller-feathered as shown by the dashed line in Figure 22. The large departure of the 8-inch drogue results from this line were attributed for the most part to errors in the definition of aircraft power requirements, in particular, the increment of power required to compensate for the relatively small drag of the 8-inch drogue. Since the incremental drag equations are especially sensitive to small power errors, subsequent tests were conducted with a 10-inch diameter drogue so that the increment of power (ΔSHP) would be larger. This decreased the sensitivity of the incremental drag equation to power error but introduced the possibility of increased error due to changes in induced drag and propeller efficiency.

The aircraft drag coefficients computed from the 10-inch drogue tests, however, fell closer to the glide test results as shown in Figure 22. In an effort to improve the results still further, the output signal of the drag load

transducer was filtered to reduce the sensitivity of the system to periodic fluctuations of drogue drag that were being encountered in flight (Figure 23). This modification resulted in an almost constant photopanel display of real-time drag as shown in Figure 24. To further investigate the effect of increasing the size of the incremental terms in Equation (9), final tests were conducted with a 12-inch diameter bucket drogue chute after a careful recalibration of the entire data system. An effort to obtain the best possible flight test data was made due to the lack of agreement between the results previously obtained with the 8- and 10-inch drogues. Although careful flying of the aircraft in smooth air apparently failed to reduce the scatter of the power data, the new drag coefficients of the aircraft computed from the 12-inch drogue data fell closer to gliding flight values than did the results of the 8- and 10-inch drogue tests. Even with this improvement, the results were unsatisfactory since the aircraft efficiency factor (e) computed from the slope of the C_D versus C_L^2 curve was greater than unity.

It should be observed from Figure 22 that correlation of the computed drag coefficients for the three test cases became worse as lift coefficient increased. This trend indicated once again the difficulty of adequately defining the power requirements of the aircraft over the lower-speed portions of the power curve where data scatter was most severe, and the extreme sensitivity of the incremental drag equation to small power-measurement errors.

Equation (8) was evaluated for the case where $E_p \neq 0$ using flight test data acquired with the three drogues and propeller efficiencies obtained from References 1 and 3. During this evaluation, it was found that the efficiencies calculated from Reference 1 for the T-34 propeller were approximately 0-to-4.0 percent points higher than those obtained from Reference 3. The effect of this difference on calculated drag may be seen in the tabulated data of Tables 2 and 3.

In view of the results obtained previously with Equation (9), it was not anticipated that the introduction of the propulsive efficiency ratio (E_p) into the calculations would provide realistic drag polars for the aircraft. However, the procedure was expected to provide some insight into the effect of neglecting propulsive efficiency changes as was done in the previous analysis.

In all cases, the propeller data revealed that the added drag increments provided by the drogues resulted in modest changes of propeller efficiency. For example, Reference 3 indicated that the added drag of the 12-inch diameter drogue resulted in an increase of propeller efficiency of 1.8 percent at 90 knots, and a decrease or propeller efficiency of 2.2 percent

at 110 knots. Changes in propeller efficiency calculated from the 8- and 10-inch diameter drogues were generally proportionally smaller as indicated by the propeller efficiency ratios of Table 2. Inspection of the calculations from Reference 1 revealed the same trends as above, except that propeller efficiency ratios were slightly higher.

Figures 25 and 26 show the effect of introducing the propeller efficiency ratio (E_p) into the calculations of aircraft drag. Because of the trend of the propeller efficiency data to increasing values of propeller efficiency ratio with decreasing airspeed, the drag coefficients obtained from Equation (8) became smaller as the lift coefficient was increased. This resulted in drag coefficients that were obviously too low at lift coefficients greater than approximately 0.50, which indicated that induced drag effects were too large to be neglected. The results also showed that induced drag effects could be expected to provide a positive contribution to the drag of the test aircraft. The inconsistency of the 8-inch drogue results shown in Figure 25 was due to the slightly lower values of propeller efficiency ratio calculated for this case from Reference 3.

Because of the unsatisfactory results obtained from Equation (8), an investigation of the effects of including the previously neglected induced drag changes in the drag calculations was attempted. An incremental form of the drag relationship in which induced drag effects are included is given by Equation (14). The evaluation of this equation must be accomplished by iterative means since the slope of the lift curve (a_0) and the span efficiency factor (e) are initially unknown. A first approximation of the lift curve slope (a_0) may be obtained from angle of attack data with the assumption that lift of the aircraft is equal to its weight. The span efficiency factor (e) may be first approximated from a drag polar based on aircraft drag calculations obtained from Equation (3) or the incremental Equation (9).

Attempts to evaluate Equation (14) in the above manner resulted in unrealistic drag values because of the difficulty of determining the incremental term ($\Delta\gamma$) in this equation. The magnitude of this term, estimated from the results obtained with Equation (8), should have varied within a range of 0.50 to -0.10 degrees. The corresponding range of values for $\Delta\gamma$ determined from flight test data was 1.25 to -0.35 degrees. It can be seen from these results that the percentage error between the measured and estimated values of $\Delta\gamma$ were quite large. Because of the sensitivity of Equation (14) to small changes in the value of $\Delta\gamma$, the unsatisfactory results obtained were believed to be due primarily to an inability to measure precisely the small changes in thrust inclination angle. The evaluation of Equations (14) and (8) did

indicate however, that changes of the induced drag of the aircraft which result from the addition of a drag increment (ΔD) may be large in comparison to the value of the drag increment itself, especially at high lift coefficients.

As a final comparison of the results obtained from the incremental drag equations, drag polars of the aircraft were calculated directly from measured power and propeller efficiencies obtained from References 1 and 3. The results presented in Figure 27 show a difference of approximately 4 percent in the values of drag coefficient calculated from the propeller efficiencies of the two different sources. The general agreement of the curves shown in Figure 27 and their proximity to the gliding-flight-test results seems to indicate that the propeller efficiencies obtained from References 1 and 3 are, at least consistent within the performance range investigated. Drag coefficients obtained from the incremental drag equations approached those obtained directly from the absolute values of propeller efficiency at small lift coefficients. This trend of the results may be seen by a comparison of Figures 26 and 27.

Since the curves of Figure 27 lie above the gliding-flight-test results obtained with the propeller feathered, the power-on propulsion system effects apparently result in an adverse interference. However, while these results appear reasonable, they are inconclusive due to uncertainty of the actual operating efficiency of the test propeller.

The problem is evidently ill-conditioned and small variations in the elements of the governing equations, particularly the incremental values, cause relatively large changes in the solutions. Thus, small errors in the flight test measurement of engine torque and drogue drag values resulted in correspondingly large changes in the calculated values of airplane drag and propeller efficiency.

CONCLUDING REMARKS

Three forms of the incremental drag equation were evaluated using flight test data obtained with three drag chutes of different size. The first form of the equation, Equation (9), was used to determine aircraft drag based solely on power and incremental drag measurements. The second form, Equation (8), included the effect of propeller efficiency changes which were determined by two different methods. Finally, the additional effects of induced drag changes were considered in Equation (10). Several conclusions and recommendations can be made on the basis of the results obtained from the incremental drag equations and from the flight test procedures that were adopted for this investigation.

Tests of drag chutes of various configuration

and size resulted in the selection of a bucket-type drogue as the most desirable drag-producing device for this investigation. The bucket drogue displayed the best stability characteristics in flight and was relatively simple to fabricate.

The incremental terms contained in the drag equations must be evaluated from generalized flight test data since exact duplication of the initial clean aircraft flight conditions is difficult and often impossible. Also, because of the sensitivity of the equations to small errors in the incremental terms, the best possible curve fits to the experimental data should be obtained to minimize errors due to data scatter.

The evaluation of the incremental drag equations indicated that Equation (9) can be expected to yield only "ball park" estimates of aircraft drag. This is because propeller efficiency and induced drag terms, which were assumed negligible, individually can have large effects on the calculations and become increasingly important as lift coefficient is increased. While the effects of induced drag and propeller efficiency terms tend to cancel, they cannot reasonably be expected to be of the same magnitude. As a result, failure to consider these terms as in Equation (9) will produce results which are, at best, only rough approximations of the actual drag of the aircraft.

Equation (8) fails to accurately predict the drag of the aircraft at high lift coefficient due to neglecting the induced drag increment, ΔD_i . Drags obtained with this equation were reasonably consistent with those calculated directly from propeller efficiency and measured power only at the lowest value of lift coefficient used in the calculations ($C_L = 0.412$). In general, this equation cannot be applied over the complete range of lift coefficients of an aircraft.

The results of the evaluation of the incremental drag equations indicate that only Equation (14) offers the potential for accurately predicting the drag of a propeller-driven aircraft over the full range of aircraft lift coefficients. Attempts to evaluate this equation with available flight test data produced unrealistic results due to apparent errors in the measured values of the increment of thrust inclination angle, $\Delta \gamma$. The successful application of the incremental drag technique would thus appear to hinge upon precision flight test measurements of this angle. Whether or not the required precision can be obtained in flight is subject to question, in that even with sensitive, reliable instrumentation, factors such as aircraft stability, pilot technique, and atmospheric conditions will influence the repeatability of the angular measurements.

In general, the results obtained from the evaluation of the incremental drag technique have shown that the method has potential.

However, the sensitivity of the equations to small errors of the incremental terms requires that data be measured in flight with a higher degree of accuracy than was accomplished in this investigation. The flight test procedure and data analysis technique developed during the investigation appears sound, but improvements of the instrumentation system are needed. This is particularly true with regard to the instrumentation for measuring propeller torque and aircraft angle of attack. The use of generalized propeller data to obtain propeller efficiency ratios for evaluation of the method should yield good approximations of aircraft drag provided these values are based on accurate measurements of aircraft power.

It is suggested that current results warrant continued investigation of the incremental drag method. Several recommendations are suggested for further investigation.

Additional flight tests should be conducted with other aircraft to verify the results found here. Resolution of the instrumentation, particularly the torque meter, could be improved by in-flight zeroing of the instrument. The scatter of the PIW-VIW curves could be reduced by utilizing an autopilot to insure constant altitude and velocity when test data is taken. After repeatability of the method is established, further tests should be conducted to determine the sensitivity of the method to small changes in aircraft drag. This would include flight with flaps partially extended or with other drag-producing items attached to the aircraft.

Other propellers should be tested in further attempts to verify the incremental technique. This would include testing at high tip speeds to investigate compressibility and blade interference effects on the method.

The incremental drag approach may have the potential to provide both profile and induced drag coefficients as accurately as those obtained from gliding flight. If the method can be successfully developed, it will represent a unique way to measure the performance of propeller-driven aircraft. The value of the method lies in its universal application to propeller aircraft of all types, and its potential use for improving the design and performance of future general aviation aircraft.

ACKNOWLEDGMENT

This investigation was supported by the Langley Research Center, National Aeronautics and Space Administration.

LIST OF SYMBOLS

A,B	Constant Coefficients Used in Least Squares Curve Fit
AF	Propeller Activity Factor
AR	Wing Aspect Ratio
a_o	Slope of Aircraft Lift Curve, 1/deg
C_D	Total Drag Coefficient
C_L	Lift Coefficient
C_P	Aircraft Power Coefficient
C_T	Thrust Coefficient
D	Total Aircraft Drag, lb
D_D	Drag of Trailing Droque or Chute, lb
D_i	Induced Drag of Aircraft, lb
E_p	Propeller Efficiency Ratio
e	Span Efficiency Factor for Wing
J	Propeller Advance Ratio
L	Lift, lb
PIW	Aircraft Power Corrected to Standard Sea Level Conditions at a Standard Gross Weight, hp
P_1	PIW for Aircraft in Clean Configuration, hp
P_2	PIW for Aircraft with an Attached Drag Device, hp
q	Dynamic Pressure, lb/ft ²
R/D	Rate of Descent, ft/sec
S	Wing Area, ft ²
SHP	Shaft Horsepower
T	Propeller Thrust, lb
THP	Thrust Horsepower
V	True Velocity, ft/sec or Knots
VIW	True Velocity of Standard Weight Aircraft at Sea Level, ft/sec or Knots
W	Weight of Aircraft, lb
α	Angle of Attack, deg

γ Thrust Inclination Angle, deg
 Δ Indicates an Increment of the Following Parameter
 η_p Propeller Efficiency
 θ Glide Angle of Aircraft in Powerless Flight, deg
 σ Air Mass Density Ratio

Single ~ and Dual Rotating-Tractor Propellers at Low Blade Angles and of Two and Three Blade Tractor Propellers at Blade Angles up to 65°, "NACA WRL316, 1943.

2. J. L. Crigler and R. E. Jaquis, "Propeller-Efficiency Charts for Light Airplanes," NACA TN1338, 1947.

3. R. Worobel, "Computer Program User's Manual for Advanced General Aviation Propeller Study," NASA CR2066, 1972.

4. R. M. Herrington, P. E. Shoemaker, E. P. Bartlett, and E. W. Dunlap, Flight Test Engineering Handbook, AF Technical Report No. 6273, 1966.

REFERENCES

1. W. H. Gray, "Wind Tunnel Tests of

TABLE 1

AIRCRAFT DRAG CALCULATIONS USING EQUATION (13): $E_p = 1$ (a) Configuration: 8-inch diameter drogue

$$P_1 = (4.8954 \times 10^{-5})V^3 + (4.0551 \times 10^3)V^{-1}$$

$$P_2 = (5.7442 \times 10^{-5})V^3 + (3.8326 \times 10^3)V^{-1}$$

$$\Delta D = (1.500 \times 10^{-3})V^2 + 3.161$$

V KTS	P_1 SHP	P_2 SHP	ΔD LB	D LB	C_D	C_L^2	η_p
90	80.744	84.459	15.311	332.778	.0683	.379	1.138
95	84.657	89.592	16.699	286.461	.0528	.305	.987
100	89.504	95.767	18.161	259.537	.0431	.248	.890
105	95.290	102.996	19.699	243.592	.0367	.204	.824
110	102.021	111.296	21.311	234.412	.0322	.170	.776

(b) Configuration: 10-inch diameter drogue

$$P_1 = (4.8954 \times 10^{-5})V^3 + (4.0551 \times 10^3)V^{-1}$$

$$P_2 = (5.4633 \times 10^{-5})V^3 + (4.4081 \times 10^3)V^{-1}$$

$$\Delta D = (2.084 \times 10^{-3})V^2 + 2.299$$

V KTS	P_1 SHP	P_2 SHP	ΔD LB	D LB	C_D	C_L^2	η_p
90	80.744	88.807	19.183	192.101	.0394	.379	.655
95	84.657	93.242	21.111	208.176	.0383	.305	.717
100	89.504	98.714	23.143	224.907	.0374	.248	.771
105	95.290	105.227	25.280	242.420	.0365	.204	.820
110	102.021	112.790	27.520	260.713	.0358	.170	.863

(c) Configuration: 12-inch diameter drogue

$$P_1 = (4.8954 \times 10^{-5})V^3 + (4.0551 \times 10^3)V^{-1}$$

$$P_2 = (5.8465 \times 10^{-5})V^3 + (4.3718 \times 10^3)V^{-1}$$

$$\Delta D = (2.809 \times 10^{-3})V^2 + 5.146$$

V KTS	P_1 SHP	P_2 SHP	ΔD LB	D LB	C_D	C_L^2	η_p
90	80.744	91.196	27.895	215.495	.0442	.379	.737
95	84.657	96.145	30.493	224.686	.0414	.305	.774
100	89.504	102.183	33.231	234.578	.0390	.248	.804
105	95.290	109.316	36.110	245.325	.0370	.204	.830
110	102.021	117.560	39.129	256.901	.0353	.170	.850

TABLE 2

AIRCRAFT DRAG CALCULATIONS USING EQUATION (12): E_p BASED ON NASA CR2066 (REFERENCE 4)(a) Configuration: 8-inch diameter drogue

$$P_1 = (4.8954) \times 10^{-5} V^3 + (4.0551 \times 10^3) V^{-1}$$

$$P_2 = (5.7442 \times 10^{-5}) V^3 + (3.8326 \times 10^3) V^{-1}$$

$$\Delta D = (1.500 \times 10^{-3}) V^2 + 3.161$$

V	P_1	P_2	ΔD	η_{P_1}	η_{P_2}	E_p	D	C_D	C_L^2
KTS	SHP	SHP	LB				LB		
90	80.744	84.459	15.311	.857	.865	1.009	276.254	.0567	.379
95	84.657	89.592	16.699	.880	.888	1.009	246.230	.0453	.305
100	89.504	95.767	18.161	.902	.904	1.002	251.836	.0419	.248
105	95.290	102.996	19.699	.915	.912	.997	253.767	.0383	.204
110	102.021	111.296	21.311	.920	.912	.991	262.792	.0361	.170

(b) Configuration: 10-inch diameter drogue

$$P_1 = (4.8954 \times 10^{-5}) V^3 + (4.0551 \times 10^3) V^{-1}$$

$$P_2 = (5.4633 \times 10^{-5}) V^3 + (4.4081 \times 10^3) V^{-1}$$

$$\Delta D = (2.084 \times 10^{-3}) V^2 + 2.299$$

V	P_1	P_2	ΔD	η_{P_1}	η_{P_2}	E_p	D	C_D	C_L^2
KTS	SHP	SHP	LB				LB		
90	80.744	88.807	19.183	.857	.870	1.015	164.860	.0338	.379
95	84.657	93.242	21.111	.880	.890	1.011	185.960	.0342	.305
100	89.504	98.714	23.143	.902	.903	1.001	222.522	.0370	.248
105	95.290	105.227	25.280	.915	.910	.995	255.973	.0386	.204
110	102.021	112.790	27.520	.920	.909	.998	298.190	.0410	.170

(c) Configuration: 12-inch diameter drogue

$$P_1 = (4.8954 \times 10^{-5}) V^3 + (4.0551 \times 10^3) V^{-1}$$

$$P_2 = (5.8465 \times 10^{-5}) V^3 + (4.3718 \times 10^3) V^{-1}$$

$$\Delta D = (2.809 \times 10^{-3}) V^2 + 5.146$$

V	P_1	P_2	ΔD	η_{P_1}	η_{P_2}	E_p	D	C_D	C_L^2
KTS	SHP	SHP	LB				LB		
90	80.744	91.196	27.895	.857	.872	1.018	186.245	.0382	.379
95	84.657	96.145	30.493	.880	.890	1.011	205.765	.0379	.305
100	89.504	102.183	33.231	.902	.901	.999	236.491	.0393	.248
105	95.290	109.316	36.110	.915	.907	.991	263.831	.0398	.204
110	102.021	117.560	39.129	.920	.900	.978	308.197	.0423	.170

TABLE 3

AIRCRAFT DRAG CALCULATIONS USING EQUATION (12): E_p BASED ON NACA GRAY CHART (REFERENCE 2)

(a) Configuration: 8-inch diameter drogue

$$P_1 = (4.8954 \times 10^{-5})v^3 + (4.0551 \times 10^3)v^{-1}$$

$$P_2 = (5.7442 \times 10^{-5})v^3 + (3.8326 \times 10^3)v^{-1}$$

$$\Delta D = (1.500 \times 10^{-3})v^2 + 3.161$$

V	P_1	P_2	ΔD	η_{P_1}	η_{P_2}	E_p	D	C_D	C_L^2
KTS	SHF	SHF	LB				LB		
90	80.744	84.459	15.311	.826	.865	1.047	160.877	.0330	.379
95	84.657	89.592	16.699	.853	.880	1.032	181.197	.0334	.305
100	89.504	95.767	18.161	.871	.886	1.017	205.991	.0342	.248
105	95.290	102.996	19.699	.883	.884	1.001	240.379	.0362	.204
110	102.021	111.296	21.311	.885	.875	.989	270.058	.0371	.170

(b) Configuration: 10-inch diameter drogue

$$P_1 = (4.8954 \times 10^{-5})v^3 + (4.0551 \times 10^3)v^{-1}$$

$$P_2 = (5.4633 \times 10^{-5})v^3 + (4.4081 \times 10^3)v^{-1}$$

$$\Delta D = (2.084 \times 10^{-3})v^2 + 2.299$$

V	P_1	P_2	ΔD	η_{P_1}	η_{P_2}	E_p	D	C_D	C_L^2
KTS	SHF	SHF	LB				LB		
90	80.744	88.807	19.183	.826	.847	1.025	150.626	.0309	.379
95	84.657	93.242	21.111	.853	.870	1.020	171.026	.0315	.305
100	89.504	98.714	23.143	.871	.880	1.010	203.135	.0338	.248
105	95.290	105.227	25.280	.883	.885	1.002	237.393	.0358	.204
110	102.021	112.790	27.520	.885	.881	.995	275.120	.0378	.170

(c) Configuration: 12-inch diameter drogue

$$P_1 = (4.8954 \times 10^{-5})v^3 + (4.0551 \times 10^3)v^{-1}$$



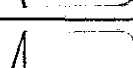
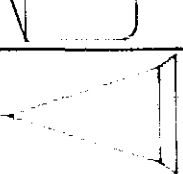

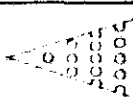
$$P_2 = (5.8465 \times 10^{-5})v^3 + (4.3718 \times 10^3)v^{-1}$$

$$\Delta D = (2.809 \times 10^{-3})v^2 + 5.146$$

V	P_1	P_2	ΔD	η_{P_1}	η_{P_2}	E_p	D	C_D	C_L^2
KTS	SHF	SHF	LB				LB		
90	80.744	91.196	27.895	.826	.855	1.035	165.082	.0339	.379
95	84.657	96.145	30.493	.853	.873	1.023	188.436	.0347	.305
100	89.504	102.183	33.231	.871	.880	1.010	217.090	.0361	.248
105	95.290	109.316	36.110	.883	.881	.998	249.209	.0376	.204
110	102.021	117.560	39.129	.885	.873	.986	287.334	.0395	.170

Table 4

DROGUE CONFIGURATIONS AND FLIGHT CHARACTERISTICS

Drogue	Configuration	Maximum Diameter, Inches	Length, Inches	C_{d_0} (Mean)*	Observed flight characteristics
8-inch diameter bucket		8	14	1.54	Spins about centerline, exhibits small circular excursions at low speeds
10-inch diameter bucket		10	14	1.26	Same as above
12-inch diameter bucket		12	14	1.25	Same as above with circular excursions of ± 0.5 ft. from centerline, occasional lateral excursions.
Surface guide		15	21.125	0.65	Spins about centerline, is unstable if not exactly circular, difficult to fabricate. Not recommended as drag device.
Tapered sock		10	30	1.31	Spins and oscillates in flight. Very unstable at speeds below 100 knots. Unacceptable as drag device. Shorter length may improve stability characteristics
Ventilated cone		10	16	0.96	Steady flight characteristics at low speeds with oscillations increasing with airspeed. An acceptable alternative to bucket-types shown above.

*Includes drag of 40-ft. tow cable, C_{d_0} based on maximum cross sectional area.

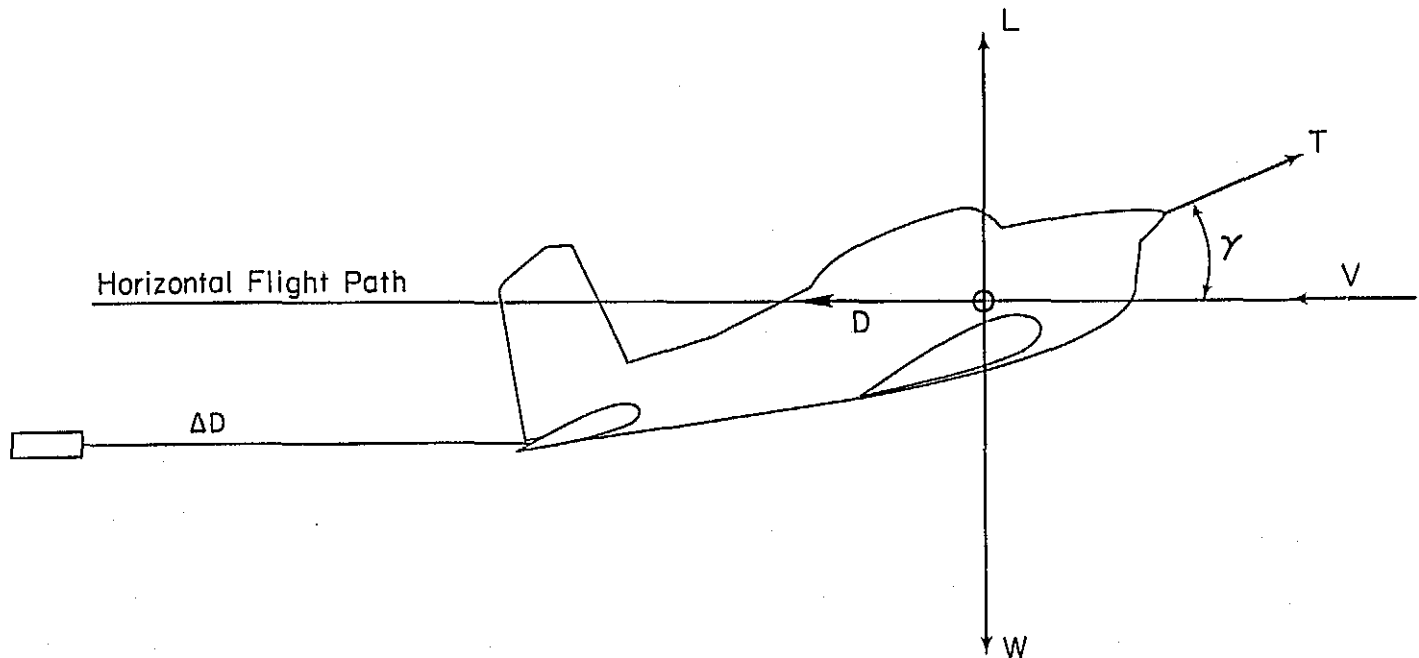


Figure 1. Aircraft Forces in Level Flight with A Trailing Drag Device

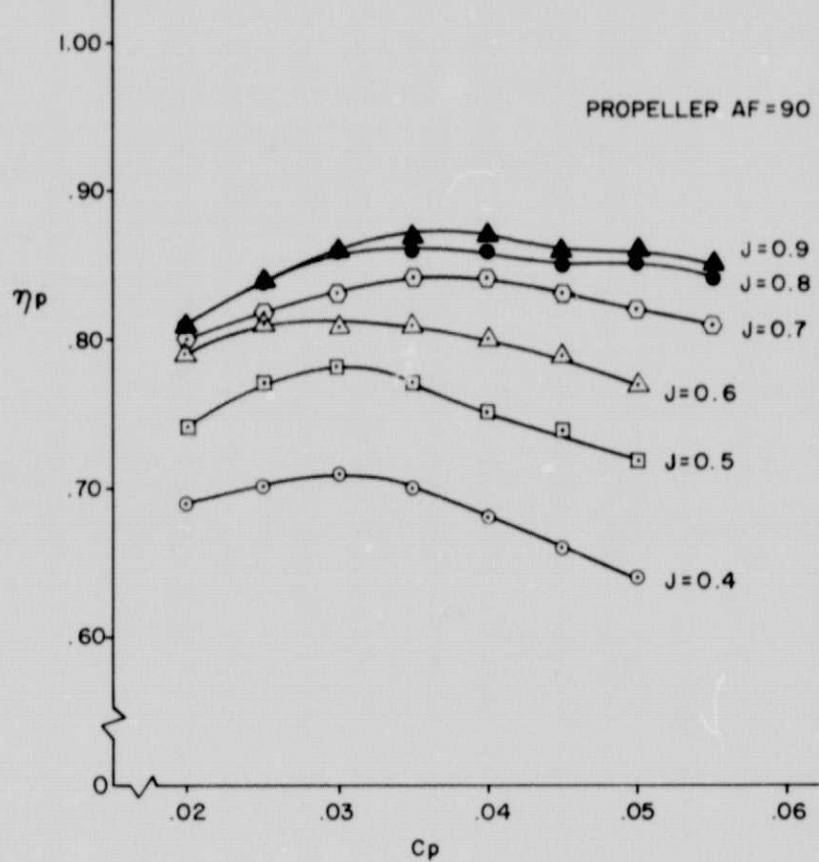


Figure 2. Propeller Efficiency Versus Coefficient of Power



Figure 3. The Test Aircraft, A Navy Model T-34B

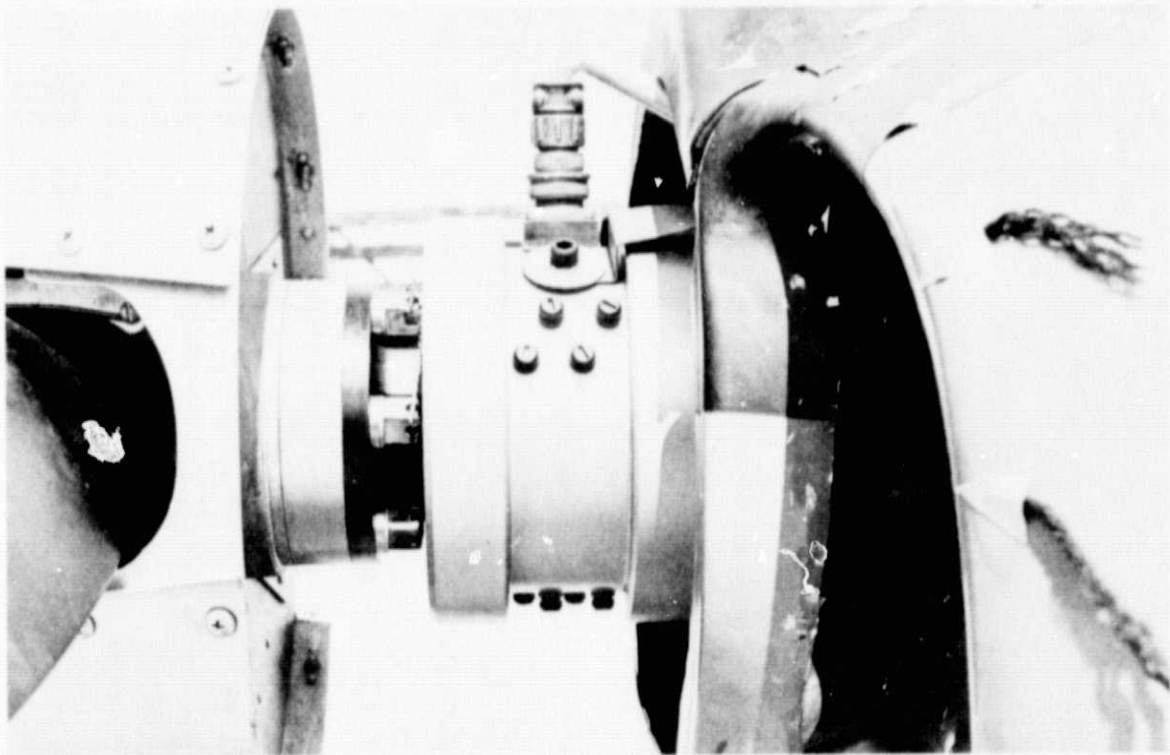


Figure 4. Propeller Torquemeter Installation on Test Aircraft

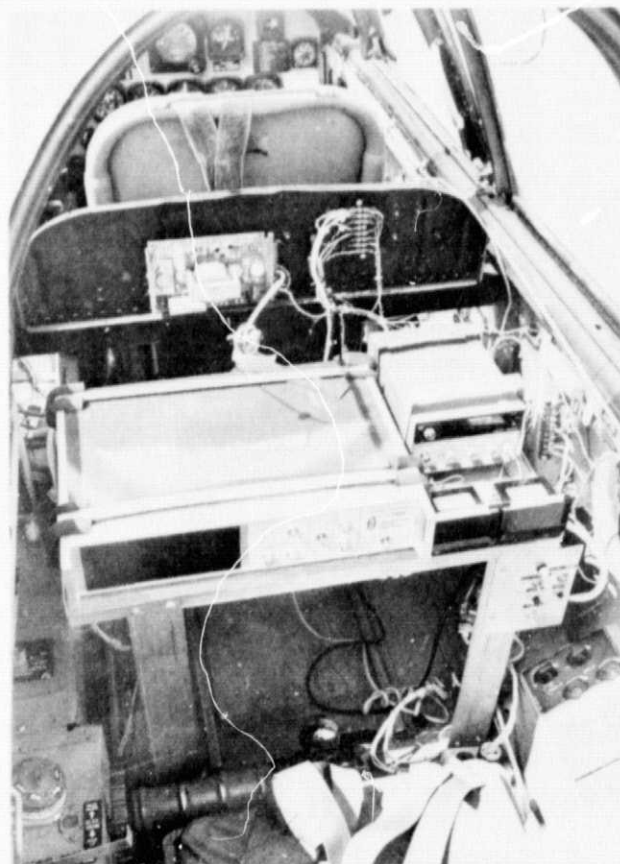


Figure 5. Rear Seat Instrumentation

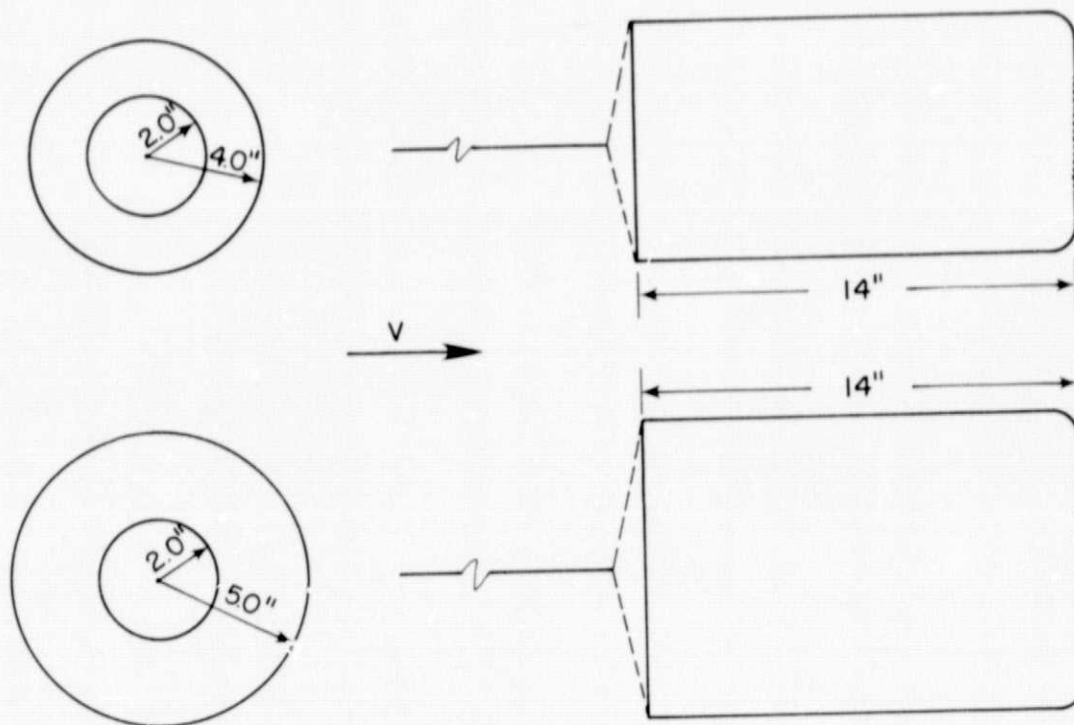


Figure 6. Schematic of 8- and 10-Inch Diameter Bucket-Type Drogues

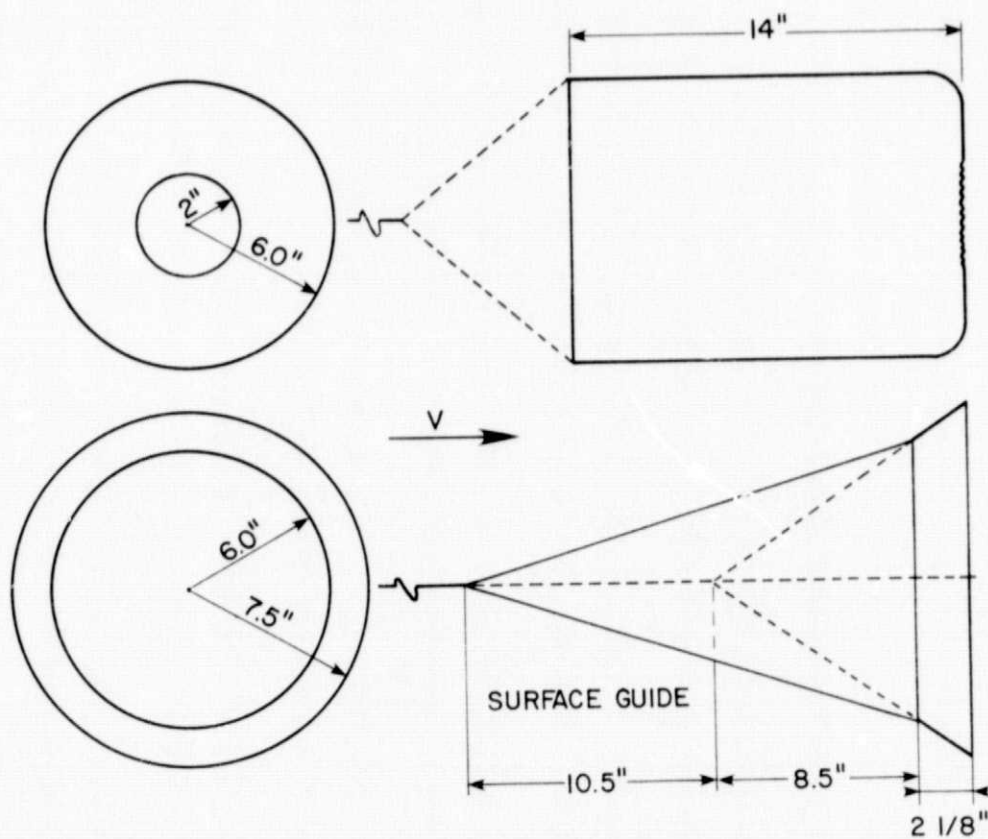


Figure 7. Schematic of 12-Inch Diameter Bucket-Type Drogue and Surface Guide Cone

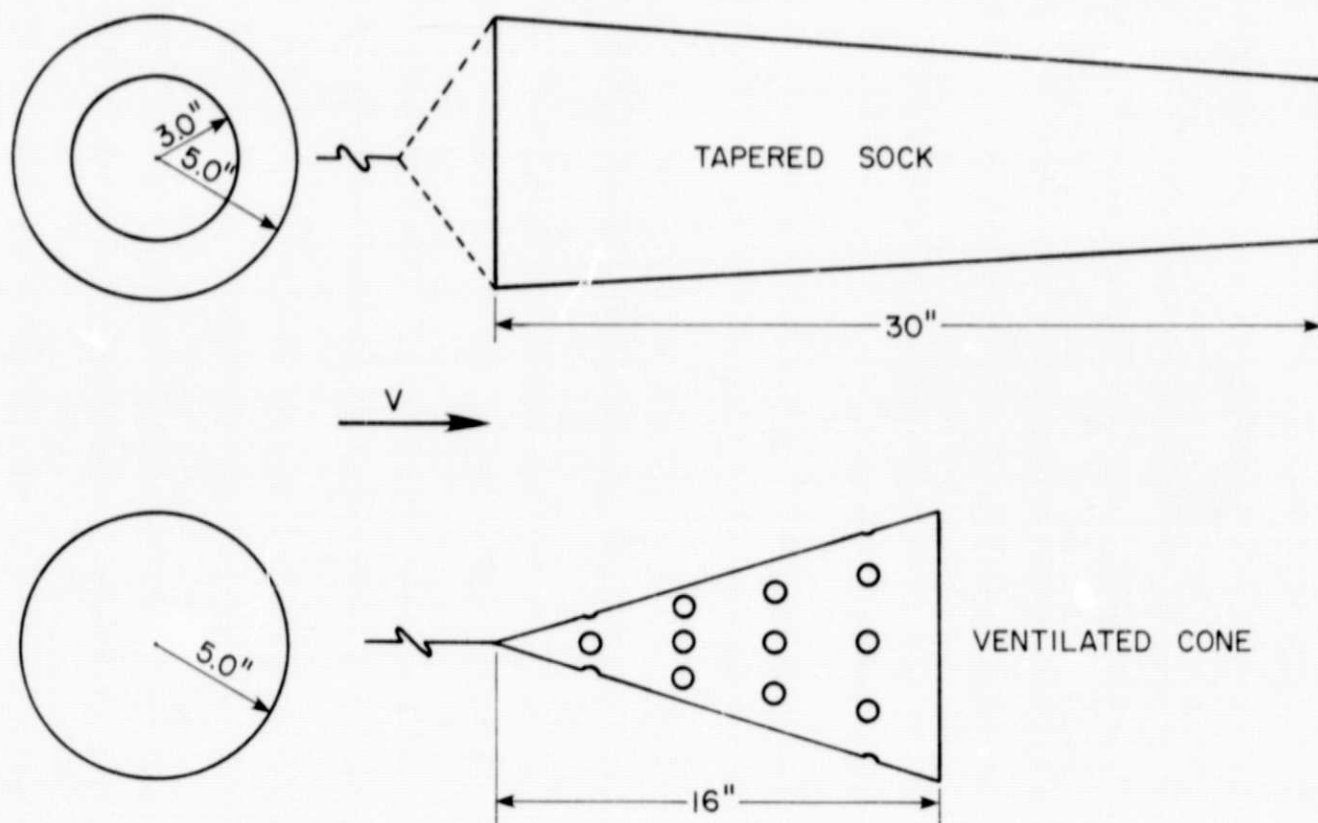


Figure 8. Schematic of Tapered Sock and Ventilated Cone Trailing Drag Devices

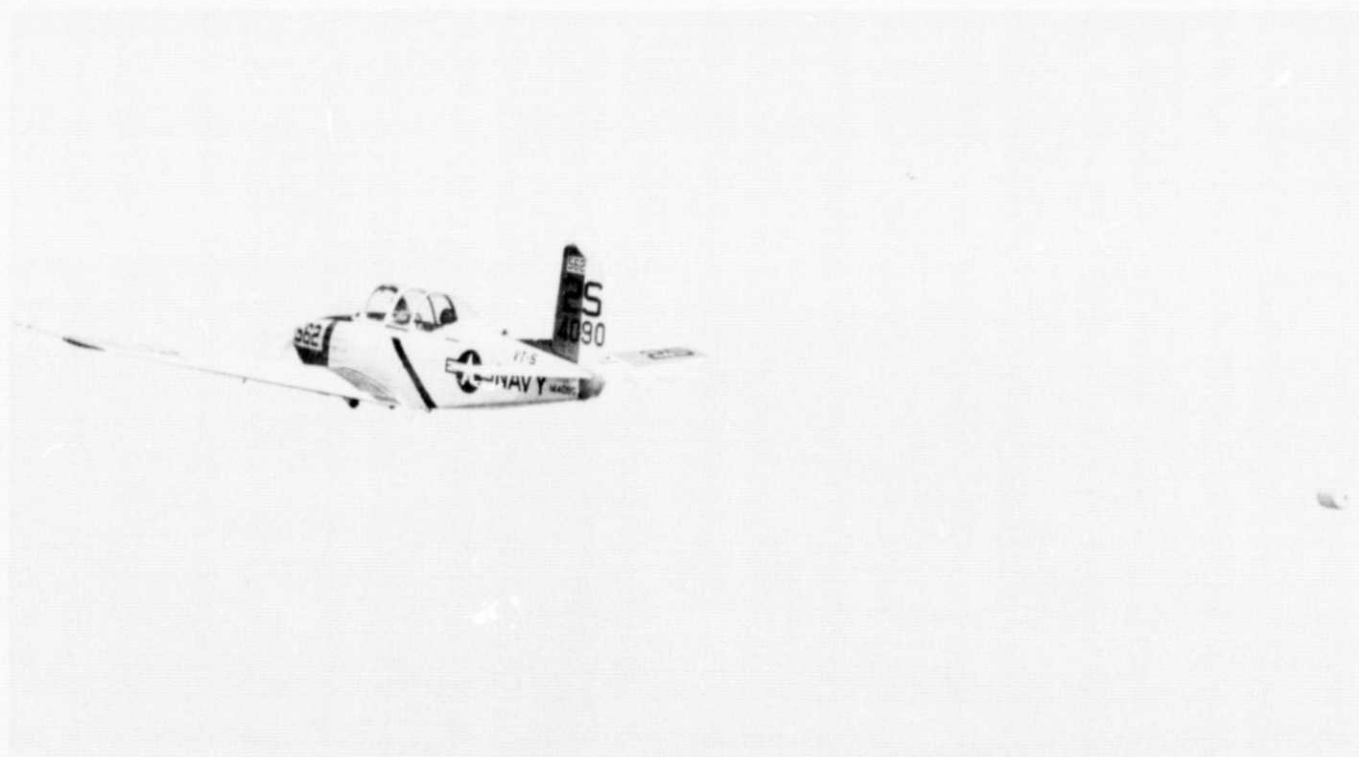


Figure 9. Test Aircraft in Flight with a Trailing Drogue



Figure 10. Load Cell Assembly in Aircraft Tail Cone



Figure 12. Wing Installation of Outside Air Temperature Probe



Figure 11. Left Wing Boom and Flying Probe



Figure 13. Photopanel Instrumentation

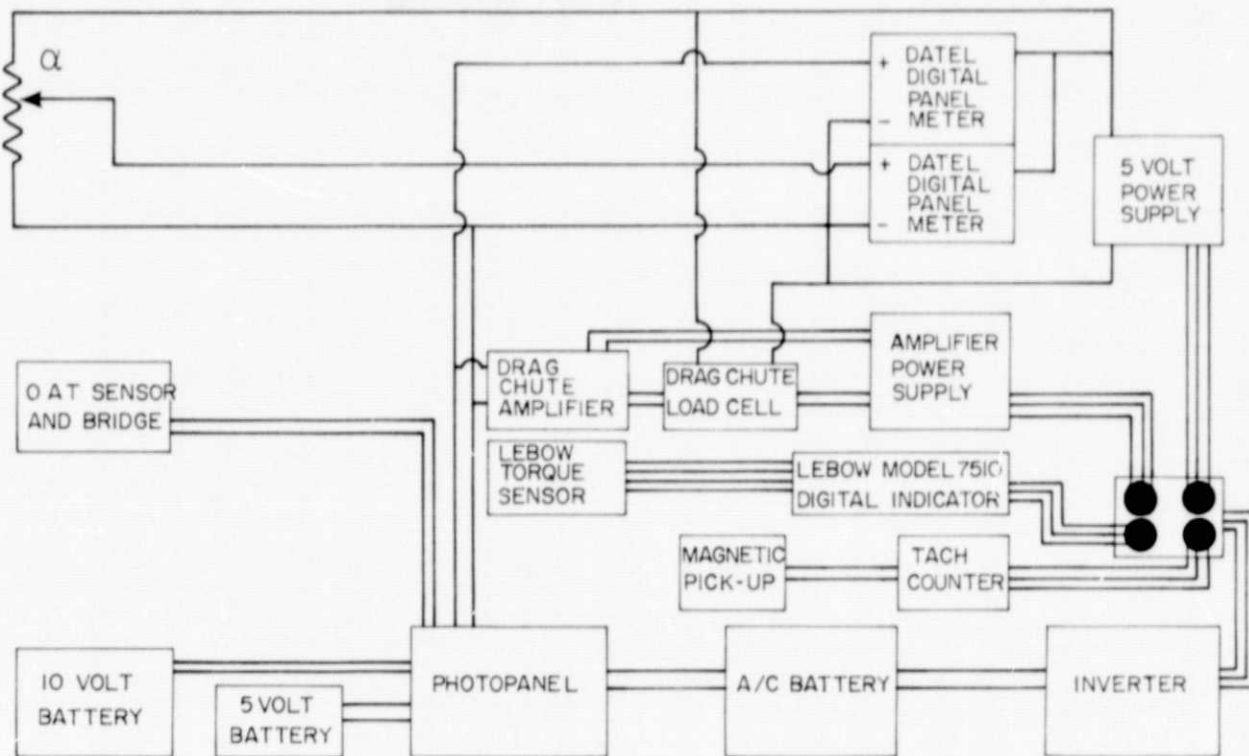
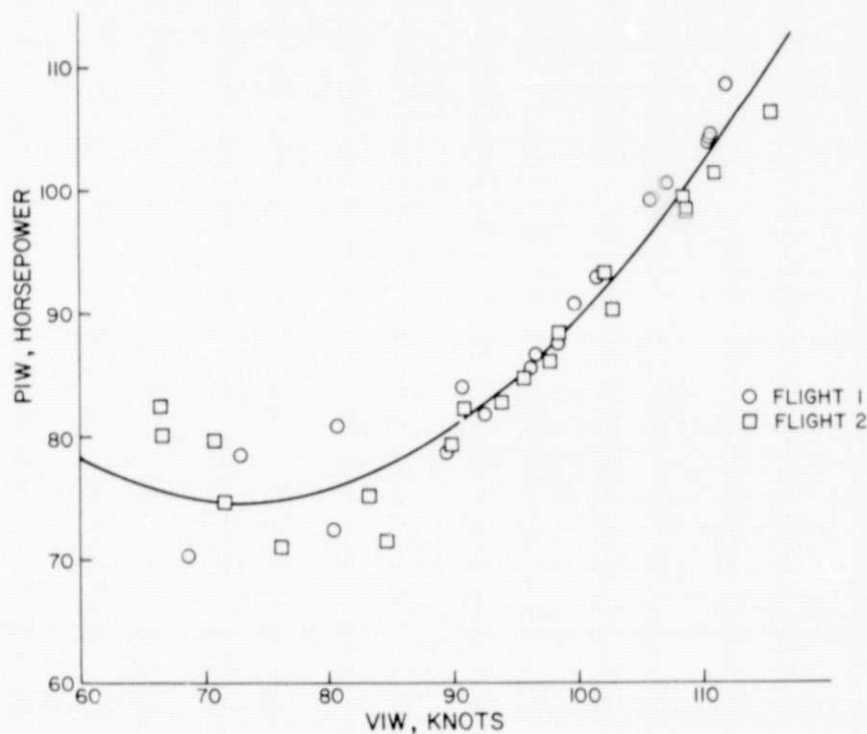


Figure 14. Schematic of Instrumentation Power System



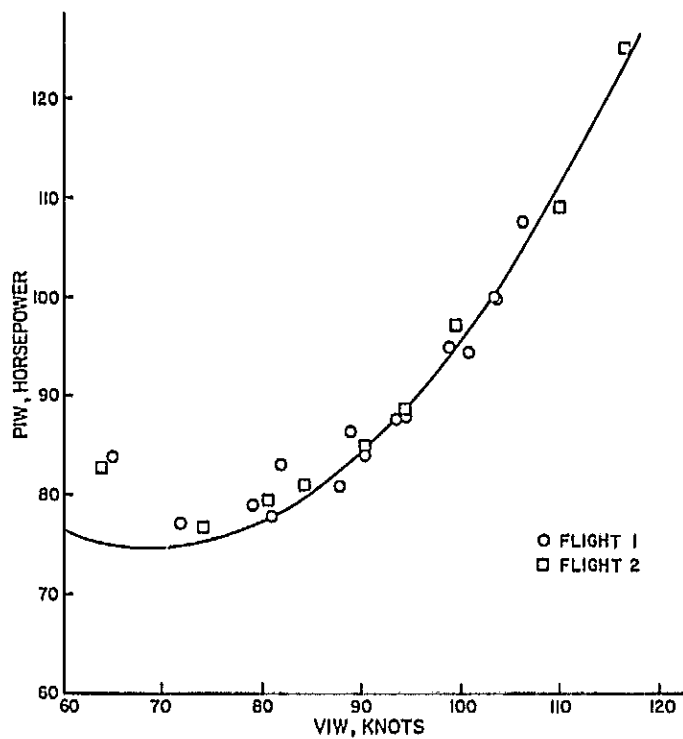


Figure 16. Generalized Power Required Data for T-34B Towing the 8-Inch Diameter Drogue

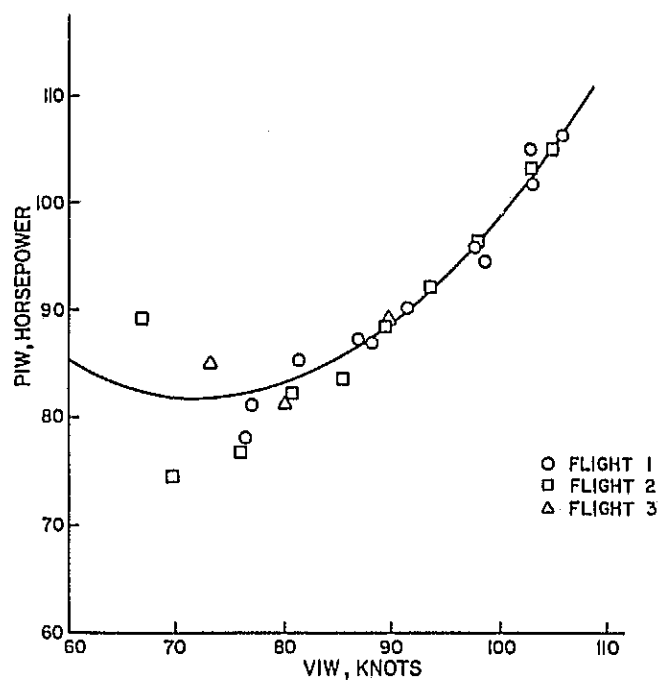


Figure 17. Generalized Power Required Data for the T-34B Towing the 10-Inch Diameter Drogue

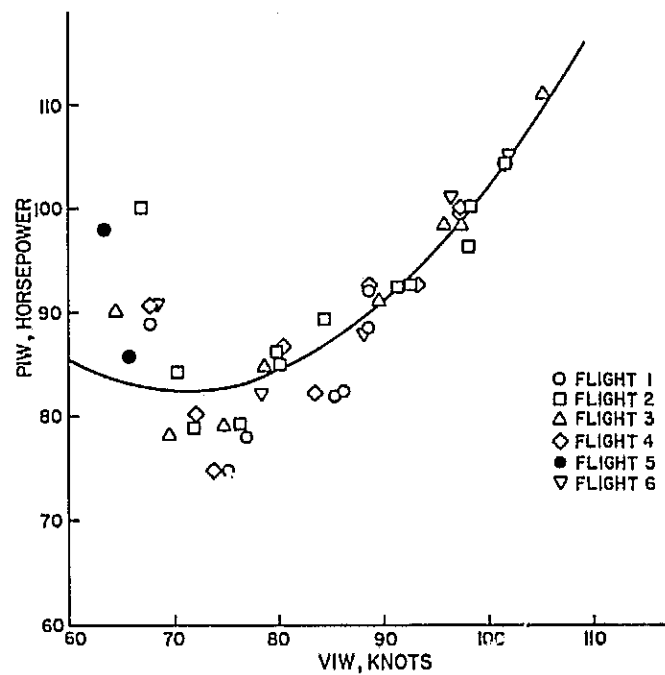


Figure 18. Generalized Power Data for the T-34B Towing the 12-Inch Diameter Drogue

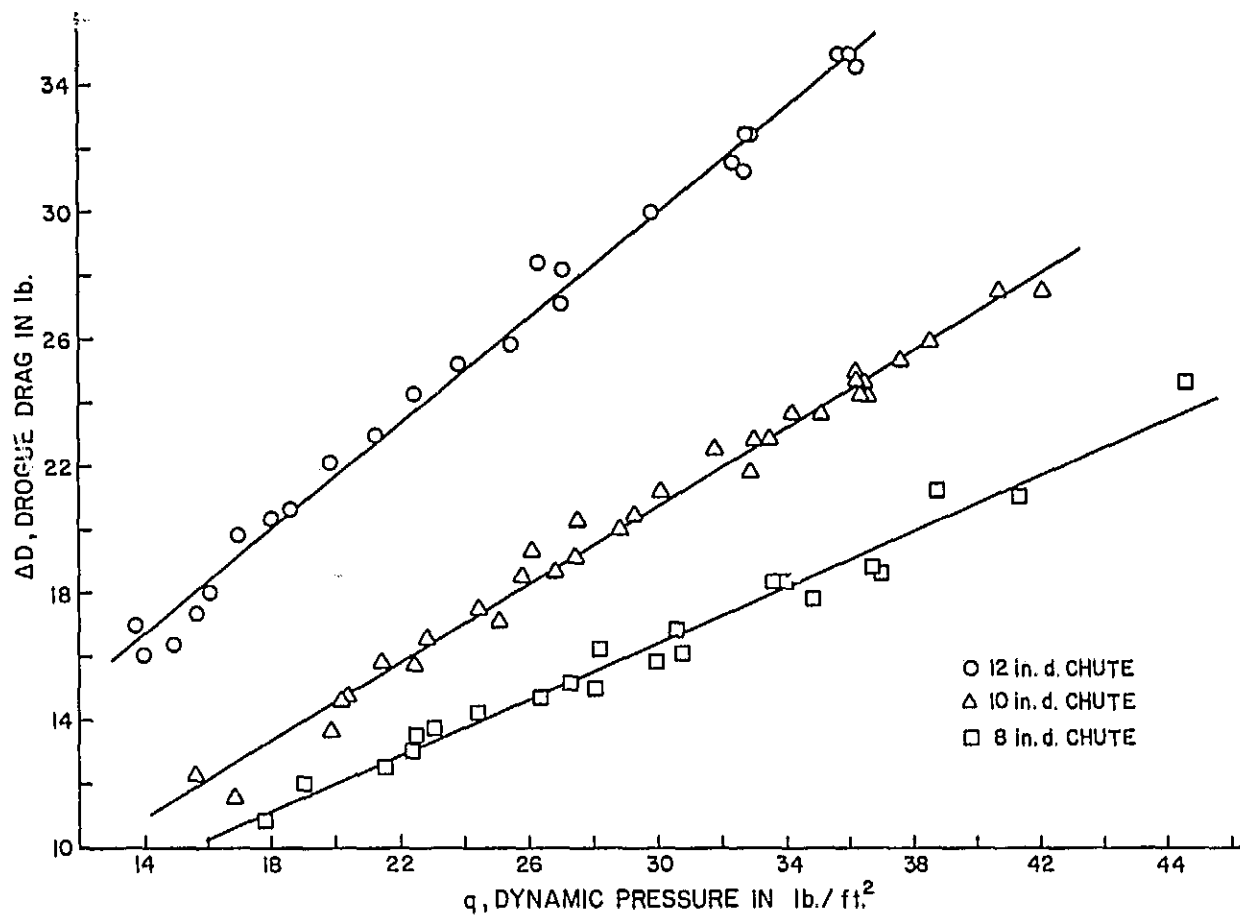


Figure 19. Experimental Drogue Drag Versus Dynamic Pressure

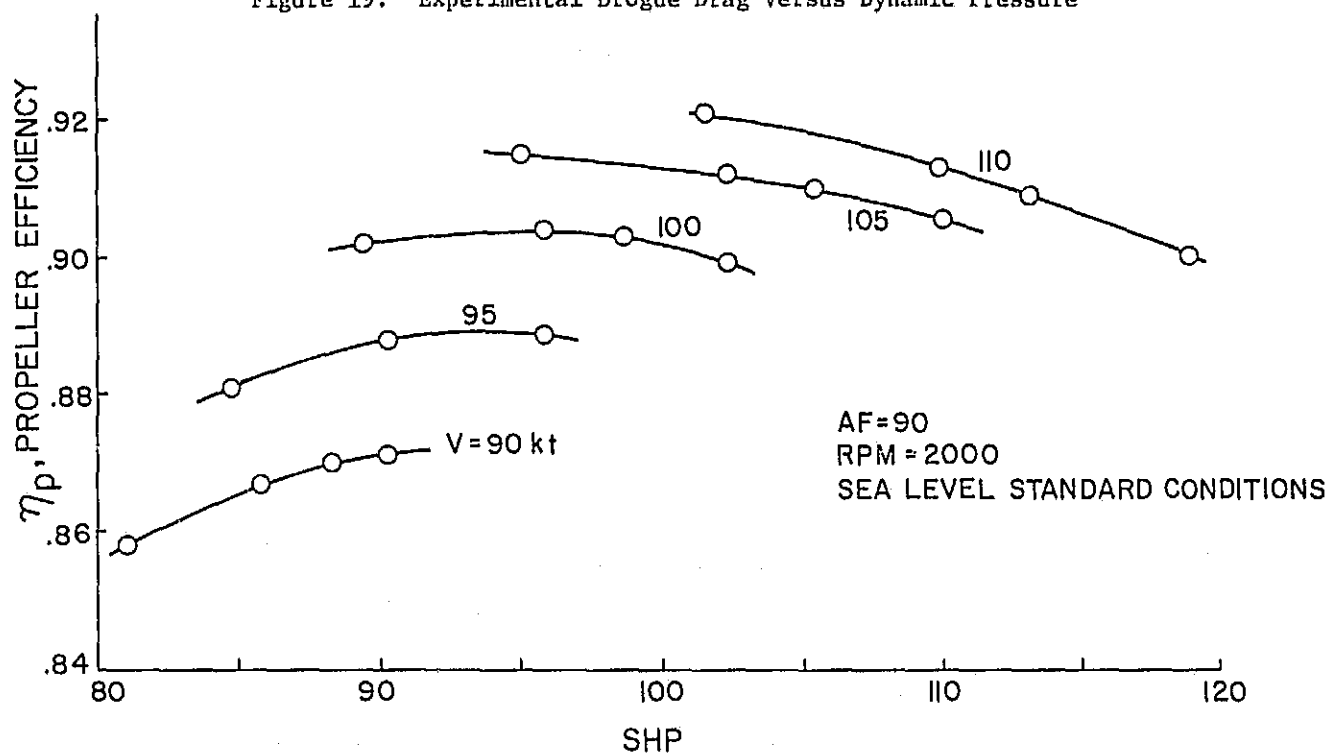


Figure 20. Propeller Efficiencies Computed from NASA CR2066 Program

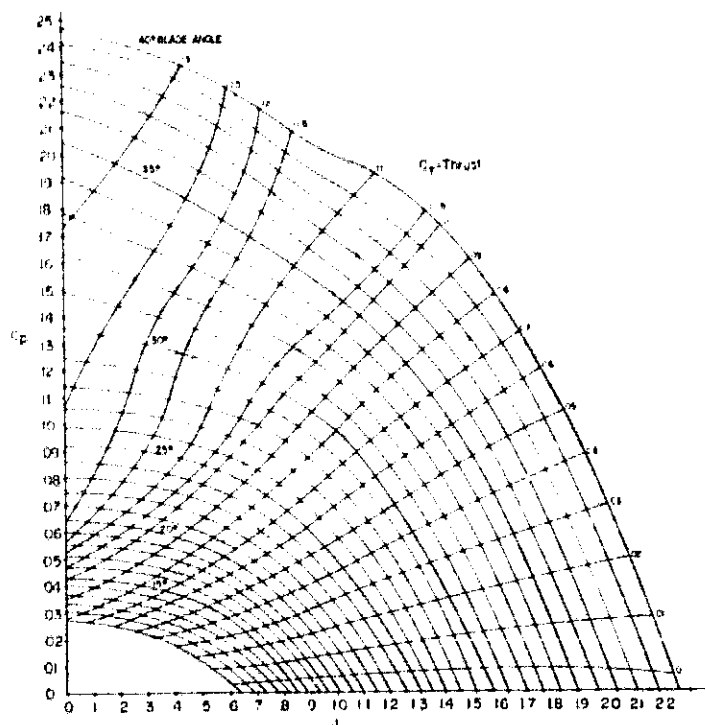


Figure 21. NACA Gray Chart. Coefficient of Power versus Advance Ratio

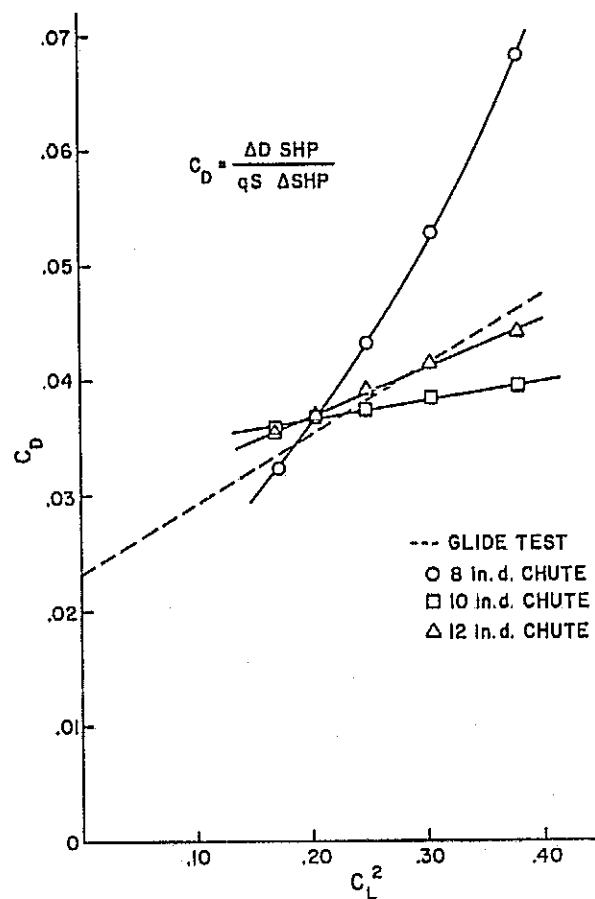


Figure 22. Results of Drag Evaluation Obtained by Use of Equation (13) with $E_p = 1$

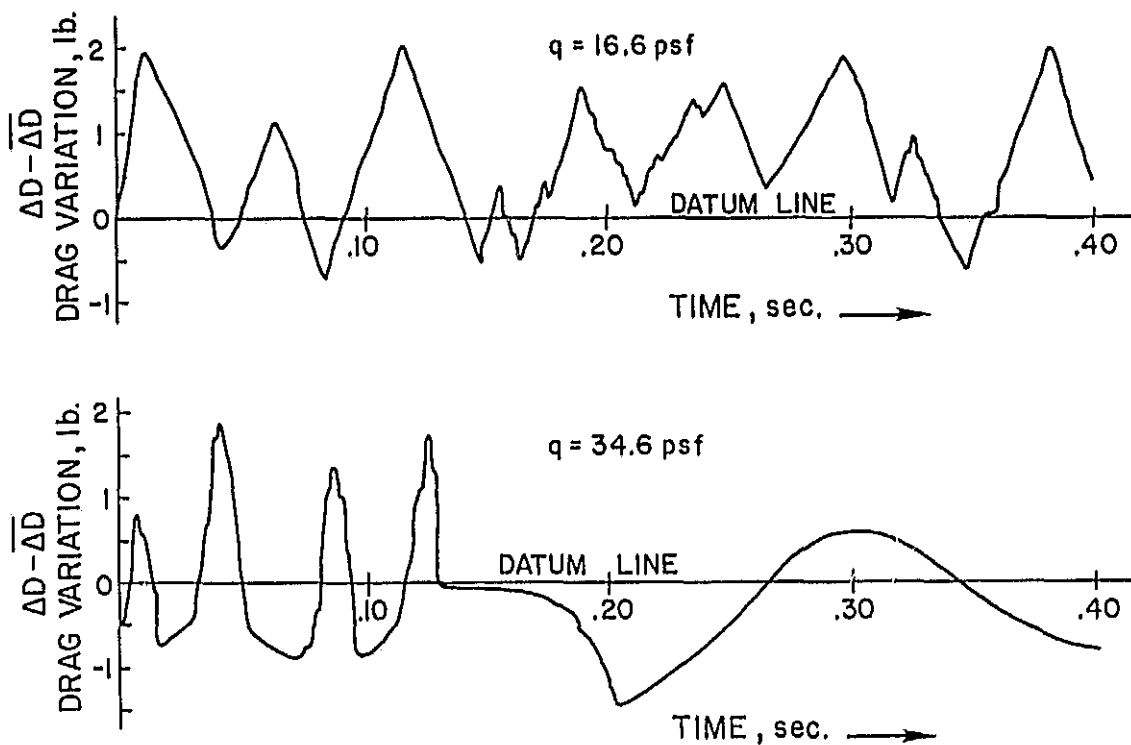


Figure 23. Drag Variation ($\Delta D - \bar{\Delta D}$) of a 12-Inch Trailing Drogue Shown by Oscilloscope Traces

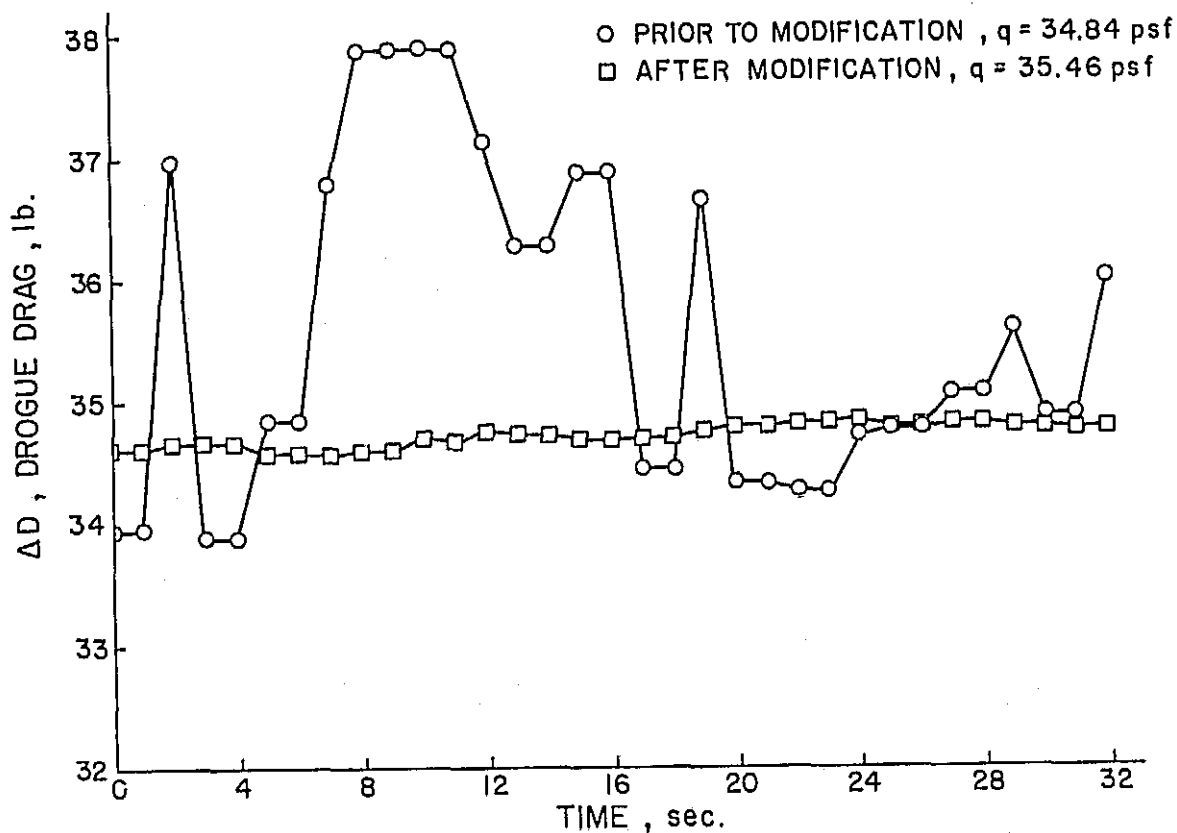


Figure 24. Effect of System Modification on the Drag of a 12-Inch Diameter Drogue as Displayed by the Photopanel

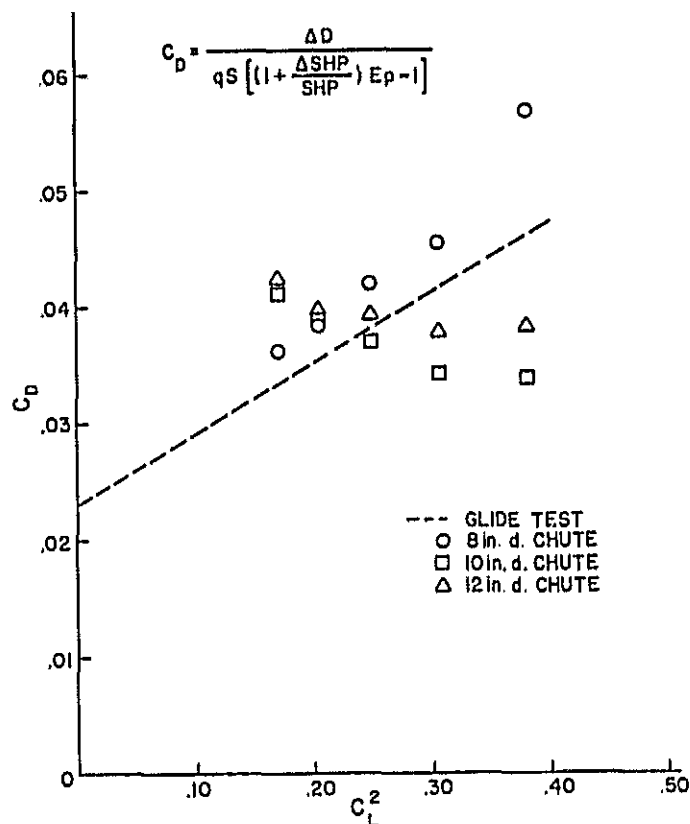


Figure 25. Results of Drag Evaluation Obtained by Use of Equation (12), E_p Calculated from NASA CR2066 Program

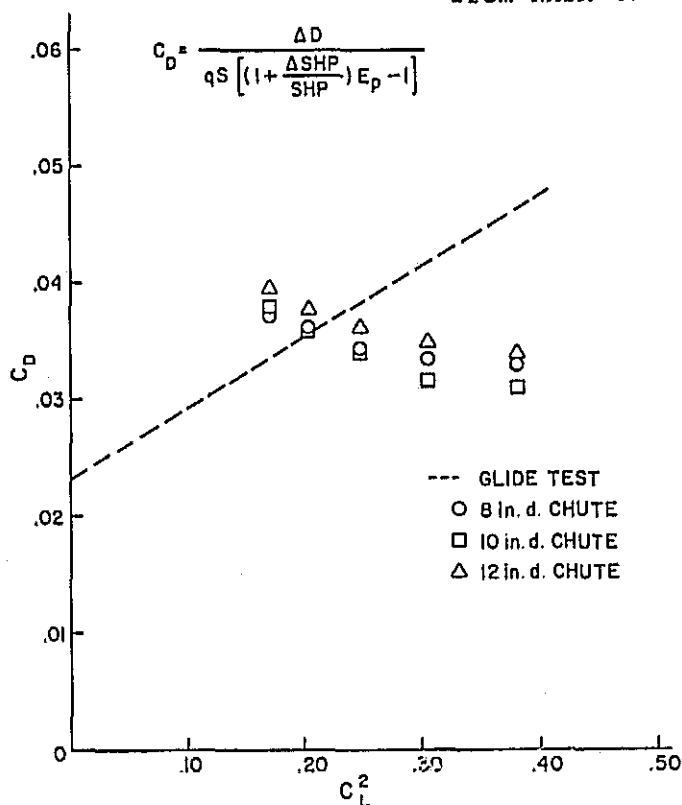


Figure 26. Results of Drag Evaluation Obtained by Use of Equation (12), E_p Calculated from NACA Gray Chart

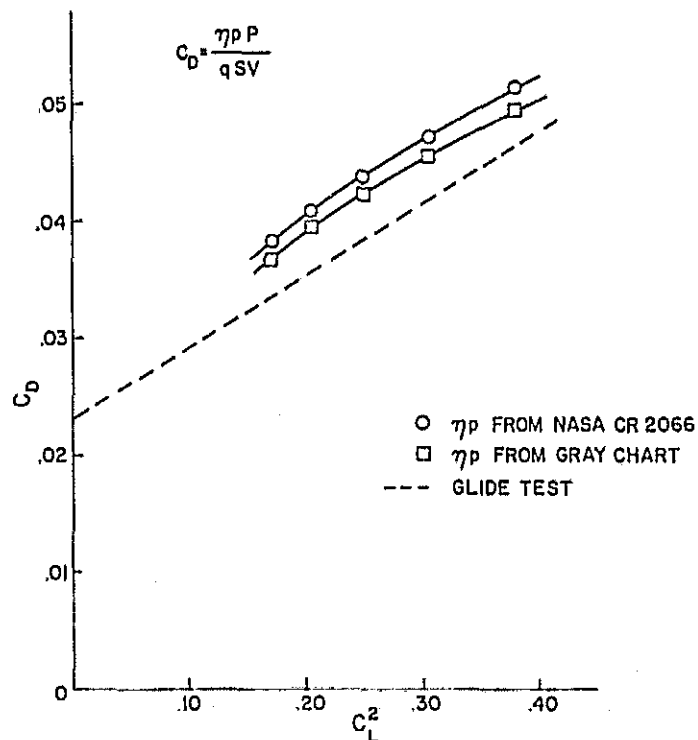


Figure 27. Drag of the Aircraft Computed from Measured Power and Two Sources of Propeller Efficiency

APPENDIX

[illegible][illegible]

ORIGINAL PAGE IS
OF POOR QUALITY

```

1* SUPPLEMENTAL RECORDING CASE
2* DISPOSITION VACATION DATA
3* DATA 1980 1981 1982 1983 1984 1985 1986 1987 1988 1989 1990 1991 1992
4* % 110 110 110 110 110 110 110 110 110 110 110 110 110
5* DATA 1980 1981 1982 1983 1984 1985 1986 1987 1988 1989 1990 1991 1992
6* % 110 110 110 110 110 110 110 110 110 110 110 110 110
7* DATA 1980 1981 1982 1983 1984 1985 1986 1987 1988 1989 1990 1991 1992
8* % 110 110 110 110 110 110 110 110 110 110 110 110 110
9* DATA 1980 1981 1982 1983 1984 1985 1986 1987 1988 1989 1990 1991 1992
10* % 110 110 110 110 110 110 110 110 110 110 110 110 110

```

```

1* SUPPLEMENTAL RECORDING CASE
2* DISPOSITION VACATION DATA
3* DATA 1980 1981 1982 1983 1984 1985 1986 1987 1988 1989 1990 1991 1992
4* % 110 110 110 110 110 110 110 110 110 110 110 110 110
5* DATA 1980 1981 1982 1983 1984 1985 1986 1987 1988 1989 1990 1991 1992
6* % 110 110 110 110 110 110 110 110 110 110 110 110 110
7* DATA 1980 1981 1982 1983 1984 1985 1986 1987 1988 1989 1990 1991 1992
8* % 110 110 110 110 110 110 110 110 110 110 110 110 110
9* DATA 1980 1981 1982 1983 1984 1985 1986 1987 1988 1989 1990 1991 1992
10* % 110 110 110 110 110 110 110 110 110 110 110 110 110

```

```

1* SUPPLEMENTAL RECORDING CASE
2* DISPOSITION VACATION DATA
3* DATA 1980 1981 1982 1983 1984 1985 1986 1987 1988 1989 1990 1991 1992
4* % 110 110 110 110 110 110 110 110 110 110 110 110 110
5* DATA 1980 1981 1982 1983 1984 1985 1986 1987 1988 1989 1990 1991 1992
6* % 110 110 110 110 110 110 110 110 110 110 110 110 110
7* DATA 1980 1981 1982 1983 1984 1985 1986 1987 1988 1989 1990 1991 1992
8* % 110 110 110 110 110 110 110 110 110 110 110 110 110
9* DATA 1980 1981 1982 1983 1984 1985 1986 1987 1988 1989 1990 1991 1992
10* % 110 110 110 110 110 110 110 110 110 110 110 110 110

```

ORIGINAL PAGE IS
OF POOR QUALITY

CORRELATION OF THE INTERPOLATED AND OBSERVED DATA IS
CORRELATION IS A THIRD ORDER OF THE FIT FOR INTERPOLATION IN ALL CASES.

CREDIT WILL IMPROVE, BUT NOT ENHANCE.

```

11 DIM I=1, J=2, K=3, L=4, M=5, N=6, O=7, P=8, Q=9, R=10, S=11
12 DIMENSION A(4), Y(4), Z(4), W(4)
13 C1 = Y(1)*WB(1)
14 C2 = Y(2)*WB(2)
15 C3 = Y(3)*WB(3)
16 C4 = Y(4)*WB(4)
17 G1 = YB(1)*C1+C2
18 G2 = YB(2)*C1+C3
19 G3 = YB(3)*C2+C4
20 B(1) = G1/G3
21 B(2) = (G1*WB(2)+G2*WB(1)+G3*WB(3)+G4*WB(4))/G3
22 B(3) = (G1*WB(2)+G3*WB(1)+G2*WB(3)+G4*WB(4))/G3
23 C(1) = 0.00
24 C(2) = B(1)
25 C(3) = B(2)
26 C(4) = B(3)
27 I = 1
28 J = 2
29 DO 5 I=1,N
30 IF(NABS(1E-WB(IP1)) GO TO 1
31 IF(1+3,1E,RO) GO TO 3
32 IP1 = NB
33 C(1) = 0.00
34 C(2) = B(1)
35 C(3) = B(2)
36 C(4) = B(3)
37 GO TO 1
38 I = I+1
39 J = I+1
40 K = I+2
41 L = I+3
42 M = I+4
43 N = I+5
44 O = I+6
45 P = I+7
46 Q = I+8
47 R = I+9
48 C1 = YB(1)*WB(IP1)
49 C2 = YB(2)*WB(IP2)
50 C3 = YB(3)*WB(IP3)
51 C4 = YB(4)*WB(IP4)
52 G1 = YB(IP1)*C1+C2
53 G2 = YB(IP2)*C1+C3
54 G3 = YB(IP3)*C2+C4
55 B(1) = (G1+G2)/G3
56 B(2) = (G1*WB(IP2)+G2*WB(IP1)+G3*WB(IP3)+G4*WB(IP4))/G3
57 B(3) = (G1*WB(IP1)+G2*WB(IP2)+G3*WB(IP3)+G4*WB(IP4))/G3
58 C(1) = B(1)+B(2)
59 C(2) = B(1)-B(2)
60 C(3) = B(3)-B(2)
61 C(4) = C1-C1
62 C(2) = (A(1)+C1+C2-C1*B(1))/G1
63 C(3) = (A(2)+C1+C2-C1*B(1))/G1
64 C(4) = (A(3)+C1+C2*B(1))/G1
65 GO TO 3
66 C(1) = C(1)
67 DO 5 J=2,4
68 C1 = C1+B(1)+B(2)
69 YB(K) = C1
70 CONTINUE
71 RETURN
72 END

```